T*ε—Bounded-Suboptimal Efficient Motion-Planning for Minimum-Time Planar Curvature-Constrained Systems

Research Thesis

Submitted in Partial Fulfillment of The
Requirements for the Degree of Master of Science
in Autonomous Systems and Robotics

Doron Pinsky

Submitted to the Senate of
the Technion - Israel Institute of Technology
Adar aleph, 5782 Haifa February 2022

Acknowledgments

This Research thesis was done under the supervision of Professor Oren Salzman from the Computer Science Department.

The generous financial help of the Technion is gratefully acknowledged.

The results in this thesis have been accepted for publication by the author and research collaborators in proceedings of conference and journal detailed below, currently under review.

- Doron Pinsky, Petr Váňa, Jan Faigl, Oren Salzman. T*ε—Bounded-Suboptimal Efficient Motion-Planning for Minimum-Time Planar Curvature-Constrained Systems, IEEE Robotics and Automation Letters (*RA-L*), 2022.
- Doron Pinsky, Petr Váňa, Jan Faigl, Oren Salzman. T*ε—Bounded-Suboptimal Efficient Motion-Planning for Minimum-Time Planar Curvature-Constrained Systems, IEEE Conference on Robotics and Automation (*ICRA*), 2022.

Contents

List of Figures

Abstract

We considered the problem of computing collision-free paths for planar curvature-constrained robotic systems in the presence of obstacles while minimizing execution time. Specifically, we focus on the setting where a planar system can travel at some range of speeds but with unbounded acceleration that can be used to model many systems. Unfortunately, planning for such systems typically requires evaluating many local time-optimal transitions connecting two configurations, which are computationally expensive. In contrast to single-speed systems, when the system can travel in a continuous range of velocities, the transitions between two configurations can not be computed analytically and have to be evaluated by numerical optimization. These optimizations are computationally expensive, and in search-based motion-planning algorithms, the transition's evaluation lasts two orders of magnitude more than any other algorithmic component. Existing methods either precompute all such transitions in a preprocessing stage or use heuristics to speed up the search without computing all those transitions, thus foregoing any guarantees on the solution quality. One may want to compute these transitions in a preprocessing stage where time is not a constraint. However in many cases this cannot be done since (i) there is no finite number of possible transitions, e.g., in a continuous space or (ii) the parameters necessary to compute the system's transitions arrive with the query, e.g., when there are dynamic environmental conditions, such as wind or ocean currents. Our key insight is that computing all the time-optimal transitions is both (i) computationally expensive and (ii) unnecessary for many problem instances. This work aims to use those insights to efficiently compute high-quality bounded-suboptimal paths. We presented an algorithmic framework, which we call T*ε, that finds a near-optimal solution by minimizing the expensive-to-compute numerical evaluations of time-optimal transitions and consequentiality the algorithm's overall runtime. It also uses a heuristic approach for computing an initial set of transitions to reduce the total number of local time-optimal transitions. We show that by computing bounded-suboptimal solutions (solutions whose cost is bounded by $1 + \varepsilon$ times the cost of the optimal solution for any user-provided ε) and not time-optimal solutions, one can dramatically reduce the number of time-

optimal transitions. We demonstrate using empirical evaluation that our planning framework can reduce the runtime by several orders of magnitude compared to the state-of-the-art while still providing guarantees on the quality of the solution, especially in dynamic environmental conditions when precomputing all time-optimal transitions in a preprocessing stage can not take place.

List of Notations

ε	Approximation factor
$v[\frac{m}{s}]$	Velocity
$u[\frac{rad}{s}]$	Turning rate
$K[\frac{m}{s^2}]$	Lateral acceleration
$v_{\max}[\frac{m}{s}]$	Maximum velocity
$v_{\min}[\frac{m}{s}]$	Minimum velocity
$\rho_{\max}[m]$	Maximum turning radius
$\rho_{\min}[m]$	Minimum turning radius
$\gamma[m]$	A path
$c(\gamma)[s]$	Cost of a path γ
s_{start}	Initial state
s_{goal}	Goal state
n	Graph node
$g(n)$	Cost from source node to n
$h(n)$	Estimation for cost from n to goal node
$\mathcal{T}$	Set of possible transitions
$c(\cdot)$	Function for evaluating the true cost of a transition
$\hat{c}(\cdot)$	Function for evaluating a lower bound for the true cost of a transition
$\kappa(\cdot)$	Indicator function
$\gamma_{\text{SP}}^{v_{\min}}[m]$	Shortest path
$\mathbf{w}$	Wind vector
$\rho_{\text{LB}}[m]$	Lower bound turning radius
$\mathcal{L}[m]$	Length of a path
$\mathbf{v_G}[\frac{m}{s}]$	Ground speed
$\mathbf{d}$	Direction vector
$\mathbf{v}[\frac{m}{s}]$	Aerial speed

1 Introduction

In this work, we study the problem of computing minimal-time collision-free paths for curvature-constrained systems with variable speed. Curvature constrains are prevalent in a variety of systems (see, e.g. [2], [3], [4], [5]). Unfortunately, determining whether a collision-free curvature-constrained path exists is NP-hard even for a planar system [6]. As a result, this continuous problem is typically discretized into a graph data structure using sampling-based [7] or search-based approaches [8], which is then queried to obtain a discrete path representing a curvature-constrained solution in the continuous space. The graph's vertices correspond to robot configurations (i.e., d-dimensional points that uniquely describe the robot's position and orientation) and edges correspond to local motions taken by the robot.

Interestingly, the computational bottleneck in these search algorithms is a frequent computation of local time-optimal robot's transitions between neighboring vertices, obtained using numerical optimization. Our key insight, depicted in Fig. 1.1, is that computing all the time-optimal transitions is both (i) computationally expensive and (ii) unnecessary for many problem instances. It is worth noting that in certain situations, these computations can be done in an offline phase. In such settings, the importance of minimizing the computation of time-optimal transitions is negligible. However, as will be shown in Sec. 2 and 5 there are conditions where those computations can not be done in advance. We introduce a novel algorithmic framework called T*ε that allows computing bounded-suboptimal solutions while reducing planning times by orders of magnitude compared to the state-of-the-art.

Our framework consists of three algorithmic components. The first component assumes that we have an efficient-to-compute *lower bound* on the cost of the optimal transition between two configurations. In Sec. 5, we demonstrate two such bounds—when the environment does not and does contain the environment drift such as wind currents. Our second algorithmic component is the A*ε-based search algorithm [9] that uses these optimal transition lower bounds, together with a user-provided approximation factor ε, to choose which edges to consider. Roughly speaking, the search attempts to use only transitions for which the true (computationally expensive) cost was computed while guaranteeing the quality bound on the obtained

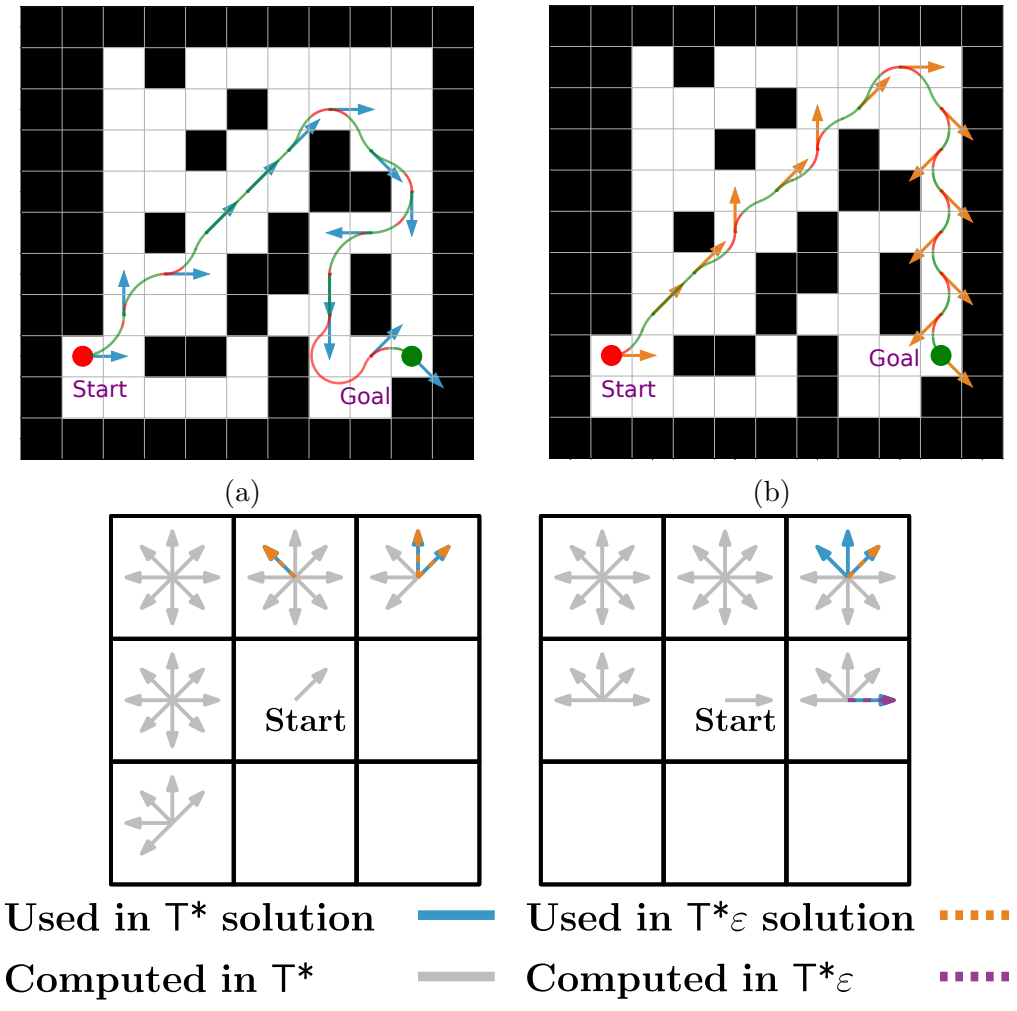

Figure 1.1: (a), (b) The time-optimal and bounded-suboptimal path obtained by T* [1] and by T*ε using an approximation factor of $\varepsilon = 2$, respectively. The red and green segments correspond to settings where the system travels at the minimum and maximum speed, respectively. The colored arrows show the orientation of each configuration in the solution. T*ε finds a solution whose cost is 7 % larger than the cost of the optimal solution found by T*, but the runtime of T*ε is faster by a factor of roughly 13×. (c) Given a start orientation (diagonal on the left or horizontal on the right) in an eight-connected grid, there are 68 unique transitions in total (after taking into account symmetry and rotation) to the adjacent grid cells. The speedup of T*ε is obtained by computing only a small subset of the time-optimal transitions that are all computed by T*. Here, T*ε computes only five transitions, four of which are used in the found path.

solution. Finally, the third algorithmic component is a heuristic approach to precompute a small set of transitions that are likely to be used in an optimal path. The goal of those three components is to guide the algorithmic framework to compute as few as possible expensive-to-compute time-optimal transitions.

Using efficient-to-compute lower bounds on the cost of local transitions is a common technique to speed up motion-planning algorithms (see, e.g., [10], [11], [12],

[13]). These are used to minimize the computation time taken to compute the cost of an edge or transition, also known as an *edge evaluation*. Typically, the edge evaluation corresponds to computing if a robot intersects an obstacle while performing some local motion (also known as collision detection [14]). Thus, the computationally expensive operation of edge evaluation is applied to each edge individually. Indeed, it can be shown that under some mild assumptions, these approaches allow minimizing the number of edges evaluated [15].

In our case, where we plan in a discretized space, i.e, the continuous search space is discretized into a lattice-based space, and there is a fixed set of transitions that can be taken from *any* given configuration. Since these transitions are computationally expensive to compute, it is natural to try and *re-use* transitions that have already been computed. The challenge is how this should be done while ensuring that the cost of the path computed is within a given multiplicative bound to the cost of an optimal path.

As we demonstrate in simulation (Sec. 5), our planning framework allows computing only a small fraction of transitions, which, in turn, allows us to reduce the runtime by several orders of magnitude compared to the state-of-the-art, especially in dynamic conditions.

The remainder of this thesis is organized as follows. A review of relevant work in the field of motion-planning for minimum-time curvature-constrained systems is presented in Sec. 2. The description and the formulation of the problem is introduced in Sec. 3. The T*ε framework is presented in Sec. 4. Empirical evaluation (in simulation) of the algorithm is presented in Sec. 5, and a conclusion and discussion about future work is outlined in Sec. 6

2 Related Work

Let continue with the review of related work on planning for minimum-time curvature-constrained systems. When the system is constrained to travel at a single speed, an optimal path connecting two configurations (i.e., two planar locations, each associated with its angular heading) can be computed analytically [16]. In this setting, an optimal path, also known as *Dubins path*, is one of six types: RSR, RSL, LSR, LSL, RLR, LRL, where R and L refer to right and left turns, respectively, and S refers to going straight. As the system travels at a single speed, the shortest and the time-optimal paths are identical.

The kinematic model considered in this work is the setting where the system can travel at some range of speeds but with unbounded acceleration (i.e., transitioning between low and high-speed can be done instantaneously). It is not hard to see that, in such a setting, the shortest path is attained by computing the optimal Dubins path, assuming that the system travels at the minimum speed (as the system can travel using the smallest turning radius possible and can thus better maneuver). However, when the robotic-system can change its velocity, the shortest path is not necessary the optimal. Computing the time-optimal path is more demanding and requires alternating between low-speed (to allow for tighter turns) and high-speed motions (to allow for faster progress).

Wolek *et al.* [17] showed that it is sufficient to consider only the two extreme speeds and identified a sufficient set of 34 candidate paths (in contrast to the six-candidate paths when the system travels at a single speed). Each candidate path contains up to five segments, compared to three in Dubins path. These can be turning right or left in maximum (bang arc) or minimum (cornering arc) speed and going forward in maximum speed. All the candidates for the time-optimal path can be seen in Fig. 2.1. However, in contrast to Dubins paths, which can be computed analytically, computing these time-optimal paths for a variable-speed system requires a numerical optimization that is (i) much more computationally expensive and (ii) may return locally optimal solutions (and not globally-optimal). Kučerová *et al.* [18] showed an efficient heuristic approach to find high-quality paths when considering time as the cost function by using multiple turning radii. However,

No.	Path Type[1]	Direction[2]	No.	Path Type	Direction
1	(B)S(B)	LSL	18	(B)S(BC)	LSR
2	(B)S(B)	LSR	19	(B)S(BC)	RSL
3	(B)S(B)	RSL	20	(B)S(BC)	RSR
4	(B)S(B)	RSR	21	(CB)(BCB)	LL
5	(BCB)(B)	LL	22	(CB)(BCB)	LR
6	(BCB)(B)	LR	23	(CB)(BCB)	RL
7	(BCB)(B)	RL	24	(CB)(BCB)	RR
8	(BCB)(B)	RR	25	(CB)S(B)	LSL
9	(B)(BCB)	LL	26	(CB)S(B)	LSR
10	(B)(BCB)	LR	27	(CB)S(B)	RSL
11	(B)(BCB)	RL	28	(CB)S(B)	RSR
12	(B)(BCB)	RR	29	(C)(C)(C)	LRL
13	(BCB)(BC)	LL	30	(C)(C)(C)	RLR
14	(BCB)(BC)	LR	31	(CB)S(BC)	LSL
15	(BCB)(BC)	RL	32	(CB)S(BC)	LSR
16	(BCB)(BC)	RR	33	(CB)S(BC)	RSL
17	(B)S(BC)	LSL	34	(CB)S(BC)	RSR

[1] B is a bang arc, C is a cornering arc and S is a straight line segment. The parentheses are used to indicate consecutive turns of the same direction.
[2] L is a left turn, R is a right turn and S means moving straight.

Figure 2.1: 34 candidates for time-optimal paths between two configurations for variable-speed system with unbounded acceleration [1].

there is no guarantee regarding the quality of these paths.

For each of the aforementioned models, motion-planning algorithms that account for environmental obstacles were introduced. These include both sampling-based approaches such as the work by Wilson *et al.* [19], search-based methods such as the work by Song *et al.* [1], and hybrid methods that borrow ideas from both motion-planning disciplines [20]. Of specific interest to the presented work is T* [1], a time-optimal risk-aware motion-planning algorithm that obtains a time-optimal solution in a discrete grid-based search space. However, it requires a time-consuming pre-processing phase where all the time-optimal transitions are computed. As our work builds upon the algorithmic foundation of T*, we describe it in Sec. 4.1. Following the exposition of T*, Wilson *et al.* [21] developed a fast, collision-free motion-finding algorithm that uses Dubins paths of various speeds to reduce the computational effort and runtime of T*. For the settings evaluated, the costs of solutions obtained by this algorithm are near-optimal, but there are no guarantees on the quality of solutions.

The aforementioned kinematic model can be extended to account for external dynamic changes such as wind or ocean currents that can be considered environment drift. For such systems with single speed, a minimum-time path can be computed similarly to the setting where no wind exists [22]. However, only two of the Dubins candidate path types have analytic solutions (RSR and LSL).

These kinematic models were used not only in the context of single-goal motion planning problems but also in the settings where the objective is to reach multiple goals [23] and further extended for some notion of rewards [24].

3 Problem Statement

Our problem formulation follows Song *et al.* [1]. Specifically, we assume a variable-speed curvature-constrained planar robotic system with unbounded acceleration. The system's dynamics is described by

$$\begin{pmatrix} \dot{x}(t) \\ \dot{y}(t) \\ \dot{\theta}(t) \end{pmatrix} = \begin{pmatrix} v(t)\cos\theta(t) \\ v(t)\sin\theta(t) \\ u(t) \end{pmatrix}. \tag{3.1}$$

Here, $(x, y, \theta) \in \mathrm{SE}(2)$ is the robot's placement and orientation, v is the robot's speed (which is considered as a control input) and u is the second control input dictating the system's turning rate via maximal lateral acceleration K that is determined for the specific system[1] as

$$|u| \leq \frac{K}{v}. \tag{3.2}$$

The speed is limited by minimum and maximum value (w.l.o.g., we assume that $v_{\max} = 1$):

$$0 < v_{\min} \leq v \leq v_{\max} = 1. \tag{3.3}$$

Thus, the system is constrained to travel between two extreme radii:

$$\rho_{\max} = \frac{v_{\max}^2}{K}, \quad \rho_{\min} = \frac{v_{\min}^2}{K}. \tag{3.4}$$

We assume that the continuous workspace is discretized to a grid according to a predefined resolution. Each cell can be categorized as *free* or *forbidden* corresponding to locations that the system can and cannot occupy, respectively. In addition, we assume that every robot motion starts and ends at the center of a cell. Specifically, at each step, the robot transitions to one of its eight neighbors and with one of eight possible orientations.

A *path* γ is a sequence of configurations where the transition between them obeys

[1] For example, $K = g \tan\varphi_{\max}$ for fixed-wing vehicles where g is the gravitational acceleration and $\varphi_{\max}$ the maximum allowed bang angle.

the system's dynamics and constraints (Eq. 3.1–3.3). It is said to be *collision free* if it only occupies free cells. The cost $c(\gamma)$ of a path γ is the step-wise cost of the transitions between any consecutive configurations in γ. It can be computed using the system velocity along γ. Namely,

$$c(\gamma) = \int_{\gamma} \frac{1}{v(\tau)} d\tau, \tag{3.5}$$

where $v(\tau)$ refers to the speed along the path segment $d\tau$.

Given start and goal configurations $s_{\text{start}}, s_{\text{goal}} \in \text{SE}(2)$, a path γ is said to be *optimal* if it (i) starts at s_{start} and ends at s_{goal}; and (ii) there is no path γ' connecting s_{start} and s_{goal} such that $c(\gamma') < c(\gamma)$. Similarly, it is said to be *bounded-suboptimal* for some approximation factor $\varepsilon \geq 0$ if it (i) starts at s_{start} and ends at s_{goal}; and (ii) for any path γ' connecting s_{start} and s_{goal}, $c(\gamma) \leq (1 + \varepsilon) \cdot c(\gamma')$.

While previous works (see, e.g., [1]) were concerned with finding optimal paths, in this work, we are interested in computing bounded-suboptimal paths for a user-provided approximation factor ε. As shown, the extra flexibility obtained by computing bounded-suboptimal paths allows us to reduce computation times by orders of magnitude with a little compromise on path quality together with a theoretic guarantee on the suboptimality bound.

4 T*ε

4.1 Algorithmic Background

As both A*ε [9] and T* [1] serve as the algorithmic foundation of our work, we provide a brief description of these two algorithms.

4.1.1 A*ε (A-star epsilon)

A*ε (also known as Focal search) [9] is a bounded-suboptimal search algorithm based on the celebrated A* algorithm [25]. Like A*, it searches in a graph by continuously expanding nodes, starting from the start node until the goal node is reached. To ensure optimality, A* orders nodes in a priority list called Open. Nodes in the Open list are ordered according to their f-value that is the sum of the cost to reach the node from the source (also known as the cost-to-come or g-value and denoted by $g(n)$ for a node n) added to a conservative estimate of the cost to reach the goal (also known as the cost-to-go or h-value and denoted by $h(n)$ for a node n). Namely for a node n, its f-value is

$$f(n) = g(n) + h(n). \tag{4.1}$$

When $h(n)$ is admissible, i.e, estimated cost-to-go is less-than or equal to the real cost-to-go, A* finds an optimal solution.

Unlike A*, A*ε also uses a so-called Focal list containing all nodes from the Open list whose f-values are no larger than $1+\varepsilon$ times the smallest f-value in the Open list. Theorem 1. in [9], shows that any sequence of nodes from the Focal list ensures that the cost of the final solution will indeed be bounded by a factor of $1+\varepsilon$ when compared to the cost of the optimal solution, is brought here. For the reader's convenience, we now repeat the original statement and proof.

Theorem 1. *A*ε *is* ε*-admissible, i.e., it always finds a solution whose cost does not exceed the optimal cost by more than a factor* $1+\varepsilon$*.*
Proof:

Let $\hat{h}$ be an admissible heuristic, n_0 the node with lowest $\hat{f}$ in OPEN*, t is a termination node (chosen for expansion and found goal), n_1 the first node on an optimal path which resides in* OPEN*, C_0 the cost of an optimal path, and $C(t)$ is the solution cost of the connecting path from the source to node t, i.e, $C(t) \triangleq \hat{f}(t) = \hat{g}(t)$.*
Since $\hat{h}$ is admissible, $\hat{f}(n_1) \leq C_0$. Now, by the fact that OPEN *is ordered according to the $\hat{f}$-values, we have that $\hat{f}(n_0) \leq \hat{f}(n_1)$, and since t is chosen from* FOCAL*, $\hat{f}(t) \leq \hat{f}(n_0)(1+\varepsilon)$. Therefore, $C(t) = \hat{f}(t) \leq \hat{f}(n_1)(1+\varepsilon) \leq C_0(1+\varepsilon)$.*

4.1.2 T* (T-star)

T* [1] builds on the approach by Wolek *et al.* [17] that allows computing an approximate[1] solution for the time-optimal transition between any two configurations in an obstacle-free space. These transitions are used to compute all possible motions for an agent in a discretized eight-connected grid. In this space, there is a finite set of possible transition types. For example, a transition can be moving from configuration $(0, 0, 0)$ to configuration $(1, 1, \pi/2)$, which corresponds to moving diagonally in the NE direction while changing the system's heading.

To this end, there are a total of $8 \times 8 \times 8 = 512$ possible transitions (eight possible start and target orientations and eight neighboring cells). However, after accounting for symmetry and rotation, there are only 68 unique transitions, Fig. 4.1 shows the all possible transitions in our setup.

After pre-computing all possible transitions, an A*-like search is used to find a minimal-cost path. In their original work, Song *et al.* [1] consider both minimal-time paths and a cost-function that balances time and the risk of colliding with an obstacle. However, we consider only minimum-time paths in this work and refer to T* as the search algorithm that optimizes this criterion.

It is important to note that it is not possible to pre-compute all transitions in an offline phase in many settings. It is because optimization-related parameters might be available only when a query is provided. For example, in the presence of wind conditions, which affect the system's dynamics and hence the transitions' computation, wind parameters are only available to the planner when a query is provided. For further details, the reader is referred to Sec. 5.

Interestingly, after extensive empirical evaluation, we noticed that: (i) pre-computing all possible transitions last two orders of magnitude more than the A*-like search; (ii) only a small fraction of all possible time-optimal transitions makes up

[1]The solutions computed are only an approximation of the time-optimal solutions since the computation is based on numerical optimizations, which may not converge to a global optimum. Thus, the optimality of T* and the bounded-suboptimality of T*ε is only with respect to (w.r.t.) the quality of the local-optimization.

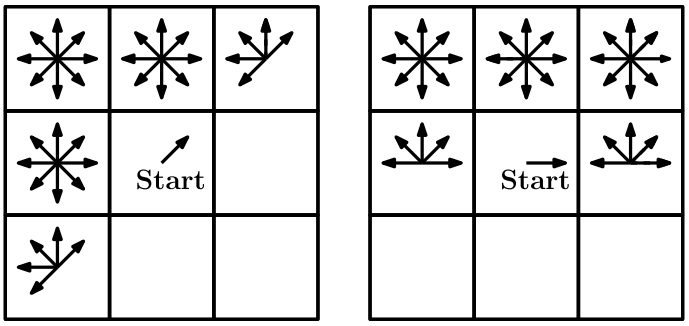

Figure 4.1: The unique transitions in an eight-connected grid with eight optional heading angles after taking into account rotation and symmetry.

an optimal path found by T*; and (iii) Dubins path computed using the minimal speed $v_{\min}$ (whose cost is a lower bound on the length of the time-optimal path) is often in the same homotopy class as the optimal path and shares a significant portion of its transitions. Fig. 4.2 shows demonstrations of (iii), notice that paths of both Dubins at minimum speed and T* usually share a large portion of their transitions. These observations are key to our algorithmic framework, which is described in the following section.

4.2 Algorithmic framework—T*ε

4.2.1 Preliminaries

Let $\mathcal{T}$ denotes a set of possible transitions. By a slight abuse of notation, we assume that we have access to two functions $c : \mathcal{T} \to \mathbb{R}$ and $\hat{c} : \mathcal{T} \to \mathbb{R}$. The first, which is expensive-to-compute, corresponds to evaluating the true cost of the transition according to Eq. 3.5. The second, which is fast-to-compute, corresponds to evaluating a lower bound on the transition cost. Namely, $\forall T \in \mathcal{T},\ \hat{c}(T) \leq c(T)$. Once the cost of a transition T is evaluated using $c(\cdot)$, the value is stored in a cache-like data structure for later use. Thus, there is no need to compute it again when evaluating the same transition later.

To this end, let $\kappa : \mathcal{T} \to \{0, 1\}$ be an indicator function corresponding to the cases where the cost of a transition T (i) has not been evaluated using $c(\cdot)$ (i.e., $\kappa(T) = 1$) or (ii) has been evaluated using $c(\cdot)$ (i.e., $\kappa(T) = 0$). We start our algorithm with the setting that $\forall T \in \mathcal{T},\ \kappa(T) = 1$.[2]

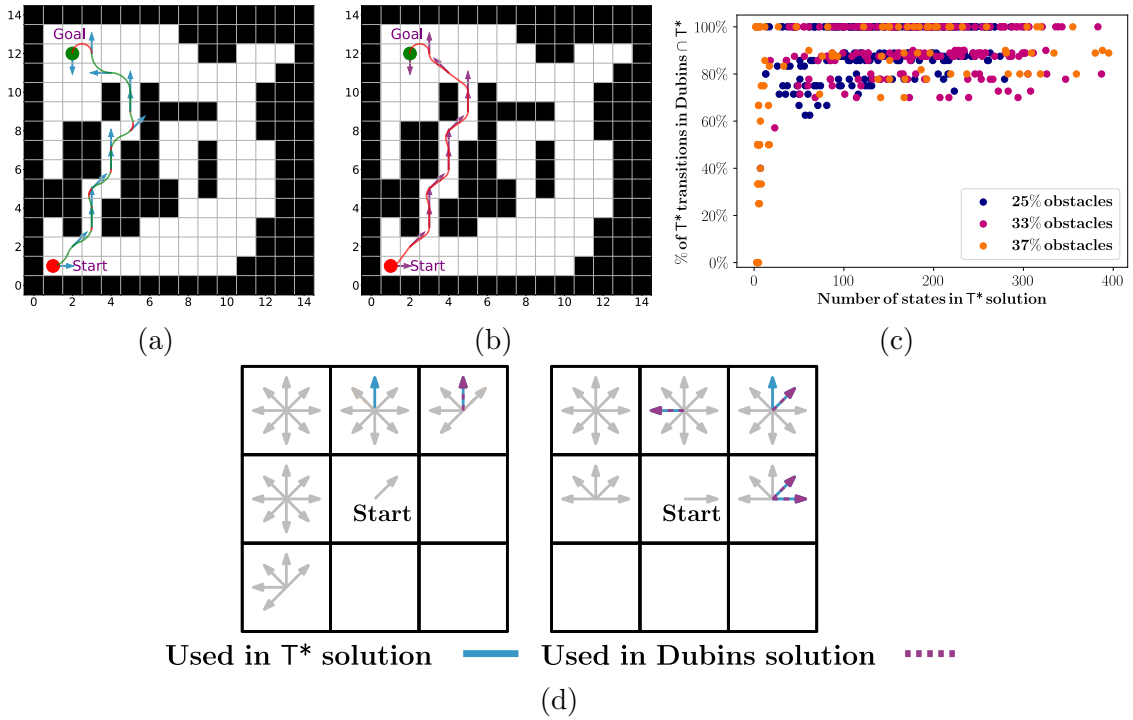

Figure 4.2: (a) The time-optimal solution obtained by T* and (b) the shortest path obtained by computing a Dubins path with minimum speed on the same setting. Notice that both paths, which are in the same homotopy class, share many transitions. (c) The number of transitions in the solution γ_{T^*} obtained by T* that also appear in the solution obtained by Dubins path of minimum speed as a function of the number of states in γ_{T^*}. The average of those mutual transitions in this evaluation of more than 550 experiments was almost 89%. (d) The transitions in the solution obtained by T* and by Dubins with minimum speed, respectively. Notice that in this example, all the transitions that appeared in the solution obtained by computing a Dubins path with minimum speed Dubins with minimum speed path are also used in the path found by T*.

4.2.2 Algorithmic Description

Our algorithmic framework summarized in Alg. 1 consists of the following two main steps.

S1: Heuristically computing the true cost for a small set of transitions.

S2: Finding a bounded-suboptimal solution while trying to minimize the number of calls to $c(\cdot)$.

In the first step **S1** (lines 1–3), we start by finding the shortest path $\gamma_{\mathrm{SP}}^{v_{\min}}$ (line 1) from s_{start} to s_{goal} that is Dubins path using the minimum speed $v_{\min}$. For every transition $T \in \gamma_{\mathrm{SP}}^{v_{\min}}$ taken along this path, we compute its true cost $c(T)$, cache it and set $\kappa(T) = 0$ (lines 2–3).

[2]The reason we chose to define κ is that we start with $\kappa(T) = 1$ for all nodes and ordering nodes lexicographically in the FOCAL list where lower means better.

Algorithm 1: T*ε

Input: map, $\boldsymbol{s}_{\text{start}}$, $\boldsymbol{s}_{\text{goal}}$, approximation factor ε
Output: bounded-suboptimal path connecting $\boldsymbol{s}_{\text{start}}$ to $\boldsymbol{s}_{\text{goal}}$

S1. compute $c(\cdot)$ for transitions in shortest path
1 $\gamma_{\text{SP}}^{v_{\min}} \leftarrow$ minimal-length collision-free Dubins path on map connecting s_{start} to s_{goal} using $v_{\min}$
2 **for each** transition $T \in \gamma_{\text{SP}}^{v_{\min}}$ **do**
3 compute $c(T)$, cache result and set $\kappa(T) = 0$

S2. A*ε-like search
4 run A*ε from n_{start} (node with state s_{start}) with OPEN and FOCAL ordered according to Eq. 4.1 and 4.3, respectively
5 **when** expanding a node n **do**
6 **if** incoming transition $n.T$ was not computed ($\kappa(n.T) = 1$) **then**
7 compute $c(n.T)$, cache result, set $\kappa(n.T) = 0$
8 **continue**
9 **if** configuration associated with the node n is s_{goal} **then**
10 **return** path associated with n
11 **for each** succesor node n' of n in map **do**
12 use Eq. 4.2 to evaluate the g-value of n'

In the second step **S2** (lines 4–12), we run an A*ε-like search to find a bounded-suboptimal path from s_{start} to s_{goal} given some approximation factor ε. We base our search algorithm on A*ε because we can use it to heuristically guide the search to expand nodes for which the incoming time-optimal transition has already been computed.

Formally, each node n considered by the search is associated with the parent node n.parent except for the start node n_{start} associated with s_{start}, which has no parent. In addition, each node stores the time-optimal transition $n.T$ used to get from n.parent to n. When expanding a node n (namely, computing successor nodes and inserting them into the OPEN list), the true cost $c(n.T)$ of the time-optimal transition leading to n is computed. However, the cost used to reach a successor node n' via transition $n'.T$ is (i) $\hat{c}(n'.T)$ if $\kappa(n'.T) = 1$ and (ii) $c(n'.T)$ if $\kappa(n'.T) = 0$. Note that for some nodes in the OPEN list, the true cost of the time-optimal transition associated with them may not have been computed. However, for all expanded nodes, the true cost of the incoming time-optimal transition is computed at some point.

To this end, if we set $g(n_{\text{start}}) = 0$ to be the cost-to-come (g-value) of the start

node, then the cost-to-come of any other node n in the OPEN list is

$$g(n) = g(n.\text{parent}) + \begin{cases} \hat{c}(n.\text{T}) \text{ if } \kappa(n.\text{T}) = 1, \\ c(n.\text{T}) \text{ if } \kappa(n.\text{T}) = 0. \end{cases} \tag{4.2}$$

The f-value of the node n (denoted by $f(n)$ and used to prioritize nodes in the OPEN list) is defined in Eq. 4.1. $h(n)$ can be any admissible estimate of the cost to reach the goal. In our setting, we use the length of the minimum speed Dubins path divided by the vehicle's maximum speed.

Recall (Sec. 4.1) that A*ε uses a FOCAL list that contains all nodes whose f-value is at most $1+\varepsilon$ the f-value of the minimal-cost node in the OPEN list. In our setting, nodes in FOCAL are lexicographically sorted using the following key:

$$\text{key}(n) = (\kappa(n.T), f(n)). \tag{4.3}$$

Thus, any node n for which $\kappa(n.T) = 0$ (i.e., the true cost $c(n.T)$ of the transition leading to n has been computed) is always prioritized before any node n' for which $\kappa(n'.T) = 1$ (i.e., the true cost $c(n'.T)$ of the transition leading to n' has not been computed), regardless of their respective f-values. Among all nodes with identical values of κ, nodes with smaller f-values are prioritized. Once a node n is chosen for expansion, the true cost of $n.T$ is computed if it has not been computed beforehand. Finally, a path is found once a node associated with the goal configuration s_{goal} is removed from the OPEN list.

Following the theoretic properties of A*ε [9] which is reviewed in Theorem 1 and using the fact that $\forall T\ \hat{c}(T) \leq c(T)$ we have the following Corollary.

Corollary 1. *Let $\varepsilon \geq 0$ and $\hat{c}(\cdot)$ be some function that bounds from below the true cost $c(\cdot)$ of any time-optimal transition. T*ε*, using $\varepsilon, \hat{c}$, and c is bounded-suboptimal with an approximation factor of $1+\varepsilon$.*

5 Simulations and Results

In this section, we report on empirical evaluation of our approach in a simulated environment inspired by Song *et al.* [1]. We start (Sec. 5.1) by evaluating our heuristic approach for computing the true cost for a small set of transitions (step **S1**). Then we continue (Sec. 5.2) to demonstrate how the lower bound $\hat{c}$ needs to be both informative (i.e., as close as possible to the real cost c) and computationally cheap-to-compute (as its main purpose is to save the computation time) by evaluating several different lower bounds that balance these two traits. We then move to compare our motion-planning approach with T* in static environmental conditions (Sec. 5.3), i.e., when the system dynamics are known before the query is provided and are independent of the specific location at which the robot resides, and in dynamic environmental conditions such as when wind currents exist (Sec. 5.4). Finally, we briefly discuss and qualitatively compare T*ε with alternative approaches to find paths that attempt to minimize the execution time (Sec. 5.5).

All experiments were run on a 3.1 GHz Intel Core i9 processor with 32 GB of memory. Benchmarks, system parameters, and C++ implementation of all the algorithms used in our work are publicly available[1]. Throughout Sec. 5.1–5.3, we test the performance of our algorithm across 100 randomly generated scenarios of 14×14 cells and using $v_{\min} = 0.5$, where for a given scenario, each cell has a probability of 25 % of being blocked, and the start and goal configurations are chosen uniformly at random while ensuring that a solution exists. When reporting algorithmic attributes, e.g., solution cost or runtime, the values represent the average across the 100 scenarios. In some cases, we also report confidence intervals that include two standard deviations from the mean. In Sec. 5.4, we provide additional information on the experiment setup.

5.1 Evaluating the Efficacy of **S1**

To evaluate the efficacy of the step **S1**, wherein we provide a heuristic approach for computing the true cost for a small set of transitions, we report the number of calls

[1] https://github.com/CRL-Technion/tstar-epsilon

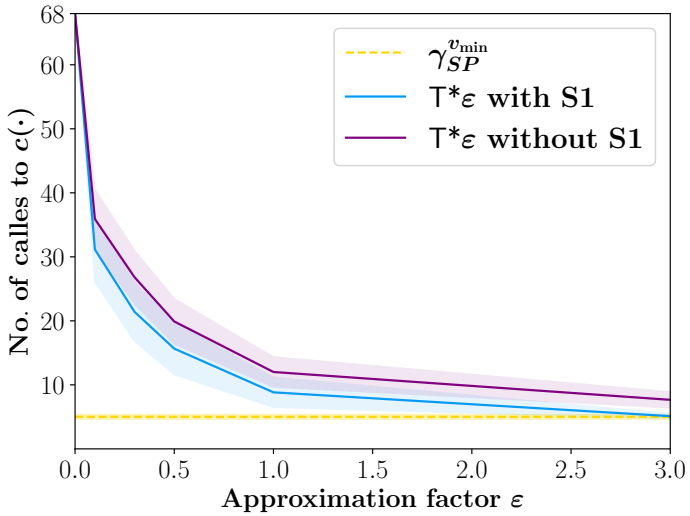

Figure 5.1: Average number of calls to $c(\cdot)$ by T*ε as a function of ε with (blue) or without (purple) the step **S1**, respectively. Recall that there are at most 68 possible transitions.

to $c(\cdot)$ by T*ε as a function of the approximation factor ε with and without this initial step (Fig. 5.1).

Observe that for values of ε larger than 0.1, using **S1** allows reducing the average number of calls to $c(\cdot)$ by roughly 10%. Moreover, in this case, for large approximation factors, the average calls to $c(\cdot)$ converges to the number of transitions in $\gamma_{SP}^{v_{\min}}$. When the step **S1** is not invoked, T*ε is not "bootstrapped" with a good set of pre-computed time-optimal and thus evaluates unnecessary transitions.

5.2 Computing Lower Bounds—Balancing Computation Time with Informative Lower Bounds

Recall that in Sec. 4.2, we assumed that we have access to $\hat{c}$—an efficient-to-compute tight lower bound on c, the true cost of the time-optimal transition. However, there is an inherent tradeoff between how informative a lower bound is (which immediately corresponds to how accurately it can guide the search) and its computation time (which can negate the effectiveness of the lower bound).

We evaluated T*ε using three different lower bounds that demonstrate this behavior: (i) Euclidean distance divided by $v_{\max}$; (ii) length of minimum-speed Dubins path divided by $v_{\max}$; and (iii) length of minimum-speed Dubins path divided by $v_{\max}$ while accounting for environment obstacles. Note that all lower bounds are divided by $v_{\max}$, thus always underestimating the true cost of a transition. In addition, they are ordered from low to high according to their computation time and how informative they are.

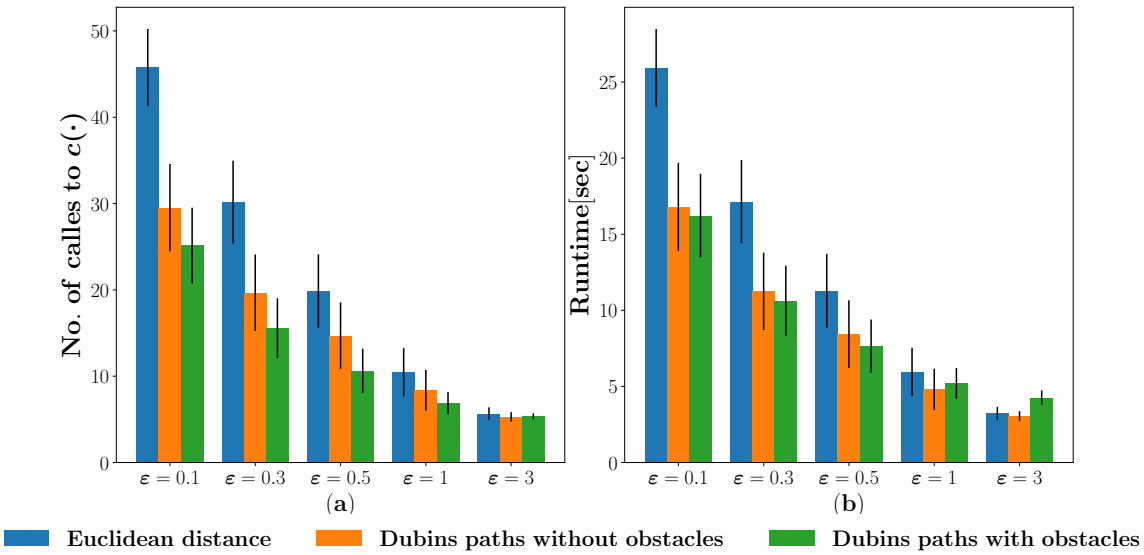

Figure 5.2: Comparing the effect of different approaches for lower bounds ($\hat{c}(\cdot)$ in Eq. 4.2) for several values of the approximation factor ε. (a) Average number of calls to $c(\cdot)$ and (b) Average running time of T*ε, respectively.

We compare (Fig. 5.2) the three lower bounds w.r.t. the number of time-optimal transitions computed by T*ε and its running time. As expected, the Euclidean distance is the least-informative lower bound, thus resulting in the maximal number of time-optimal transitions computed for all values of ε. Moreover, even though it is efficient-to-compute, it does a poor job in guiding the search, and thus the runtime is high. Computing Dubins path while accounting for obstacles is more informative but also more expensive-to-compute. It does result in the smallest number of calls to $c(\cdot)$ but has longer running times when compared to using Dubins paths that do not account for obstacles. The latter also has a comparable number of calls to $c(\cdot)$. Thus, we use lower bound Dubins paths without obstacles in the rest of the evaluation.

5.3 Motion Planning in Static Environmental Conditions

We compare T*ε with T* in static environmental conditions, i.e., where the system dynamics are invariant to the robot's placement and orientation in the scenario. As we can see in Fig. 5.3c, computing time-optimal transitions dominate the running time of all algorithms. If the system dynamics are known in advance, these can be pre-computed in an offline step by T*, and it outperforms T*ε for all ε by a factor of between 60× and 290×. However, if we account for this preprocessing time, T*ε dramatically reduce the run time by a factor ranging between 8× and 15×. It is worth noting that in either case, T*ε finds a solution with an average cost that is

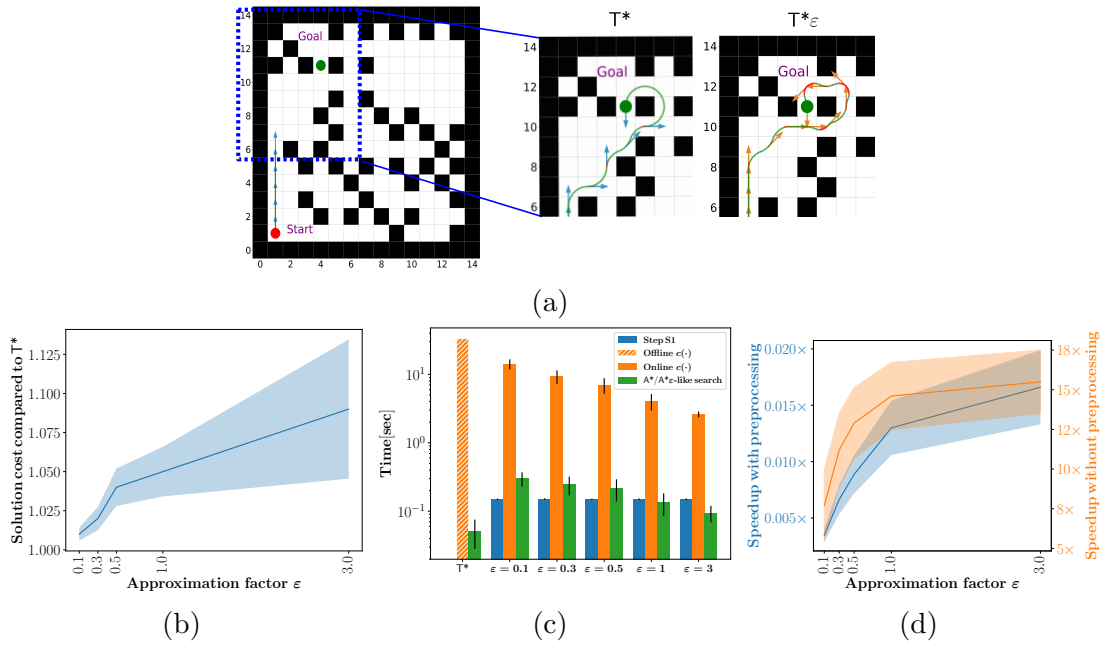

Figure 5.3: Comparison of T* and T*ε in static environmental conditions over 100 randomly chosen start and goal configurations. (a) Solution found by T* and by T*ε with $\varepsilon = 3$ for one representative experiment. The beginning of the solution found by both algorithms is identical, while the end differs and is highlighted on the right-hand side. (b) Average solution cost of T*ε compared to T* as a function of ε. (c) Breakdown of the running time of T* and T*ε for different values of ε. (d) Speedup in running time of T*ε over T* obtained with and without pre-computing all time-optimal transitions.

much lower than the guaranteed suboptimality bound.

5.4 Motion Planning in Dynamic Environmental Conditions

In the previous section, we considered static environmental conditions and showed that using an approximation factor allows reducing T*ε's planning times dramatically. However, if the system's dynamics are known in advance, T* may perform all its computationally-expensive operations in a preprocessing stage. In contrast, this is not the case when the system's dynamics are not known in advance. It can be due to changes in the maximal speed that the system can take (due to, e.g., payload changes of the system or regulatory changes happening just before a query is received) or due to dynamic environmental conditions such as wind currents whose magnitude and direction is known only when a query is received. We use the latter case to demonstrate the efficacy of T*ε. In particular, we assume that the magnitude of wind currents is uniform across a given scenario.

It is worth noting that this dynamic setting, analyzed by Techy and Woolsey [22], can be seen as a generalization of the setting described in Sec. 3 and by Mittal et

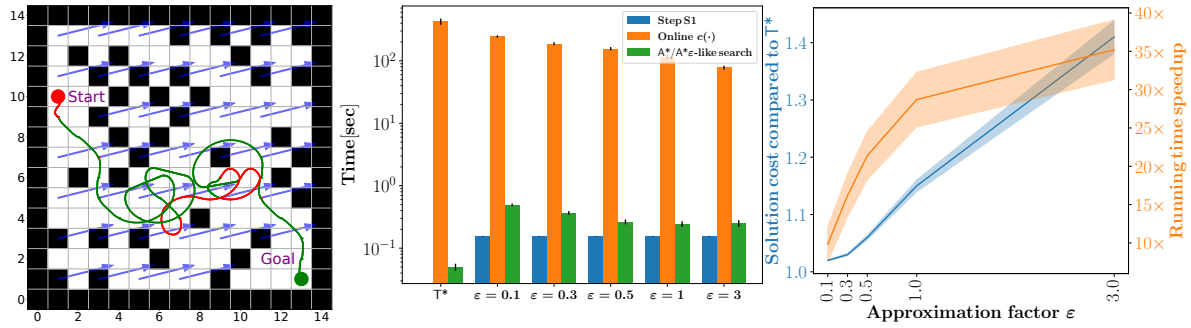

(a) (b) (c)

Figure 5.4: Comparing T* and T*ε in dynamic environmental conditions where the magnitude and direction of wind currents (blue arrows) are given at the query time. (a) A representative solution obtained on one randomly-generated map with randomly-generated start and goal configurations, wind conditions, and minimum velocity $v_{\min}$. (b) Running time breakdown of T* and T*ε for the selected values of ε. (c) Average solution cost compared to the cost of the optimal solution and speedup in running time as a function of ε.

al. [26]. To account for this more involved dynamic setting, we first note that one cannot use rotation and symmetry between transitions to reduce the total amount of unique transitions. Thus, in this setting, the total number of time-optimal transitions is 512. Moreover, this requires an adaptation of how time-optimal transitions are computed (see Appendix for a description of the new model). This adaptation, based on the code for computing time-optimal transitions [17], is publicly available[2]. The second notable change is that computing lower bounds (namely, calling $\hat{c}$, requires some care, and the modifications are detailed in Appendix.

For dynamic environmental conditions, we used the same randomly generated scenarios as described earlier. For each such scenario, we generated 10 instances with varying wind and minimum velocity values. In particular, we sampled wind conditions from $|\mathbf{w}| \in [0.14, 0.41]$ and minimum velocity values $v_{\min} \in [0.4, 0.9]$. In total, we ran 1000 experiments and the averaged results appear in Fig. 5.4. The most computationally demanding component in both T*ε and T* is still computing the time-optimal transitions, which requires two orders of magnitude more time than any other algorithmic component. However, we observe that the approximation factor allows for a dramatic reduction of the running time with a little compromise on the quality of the solution. For example, as it can be seen in Fig 5.4c, using $\varepsilon = 1$, T*ε guarantees a solution whose cost is at most twice $c(\gamma^*)$ the cost of the optimal solution, but returns a path whose average cost is no more than $1.15 \cdot c(\gamma^*)$. It is done while obtaining a speedup in run time by an average factor of 28×. In general, as depicted in Fig. 5.4c, increasing ε results in a dramatic running time improvement

[2] https://github.com/CRL-Technion/Variable-speed-Dubins-with-wind

at the cost of slightly lower solution quality.

5.5 Discussion—Alternative Approaches

Wilson *et al.* [21] reduced computational effort by allowing the system to follow Dubins paths but using several radii, and evaluated this approach when using three different radii. This heuristic approach reduces runtime, produces near-optimal solutions but with no guarantees regarding their quality. From our comparison of T*ε and Wilson's model in static environments, we found that running times are faster by several orders of magnitude, but path costs are larger by an average of 18 %. However, when evaluating their approach in windy conditions, the speedup in running time is comparable to T*ε (as local transitions cannot be computed analytically and a computationally expensive root-finding problem needs to be solved [22]), and the quality of paths remain higher (again, with no formal guarantees).

An alternative approach is to compare our work with the approach by Mittal *et al.* [26] that specifically accounted for efficient computation of paths in dynamic environments. However, the main objective of their approach is online motion-planning under ocean currents, and no importance was given to the quality of paths. When comparing T*ε with their approach on representative environments, the path quality obtained by T*ε was higher (lower execution times) by a factor of more than 2.7×.

6 Conclusion and Future Work

In this work, we presented T*ε, a novel algorithmic framework for efficiently finding bounded-suboptimal solutions for time-optimal motion-planning. This is done by minimizing the number of computations of time-optimal transitions used by the system. When one cannot pre-compute the time-optimal transitions in advance, this reduces the planning times by orders of magnitude compared to the state-of-the-art.

Future work includes adapting our work for efficient re-planing (e.g., when the wind changes while the system is in motion or dramatic payload changes during trajectory execution). Here, we plan to adapt LPA* [27] to account for minimizing the number of transitions used.

Choosing the appropriate approximation factor in bounded-suboptimal algorithms such as weighted A* [28] and T*ε is non-trivial and application dependant, and we believe it is out of the scope of this work. Having said that, we wish to give some guidelines and approaches from a practitioner's point of view.

Without any additional information, a user should choose the largest approximation factor acceptable from an application point of view. For example, if we are willing to accept paths whose cost is at most 10% longer than the optimal cost, we choose an approximation factor of $\varepsilon = 0.1$. Clearly, this is over-conservative as in practice (and as demonstrated empirically in our experiments), the path quality is likely to be much closer to optimal. We can gain more computational benefits by choosing a larger approximation factor.

An immediate next step to tackle the problem of choosing the approximation factor ε is to turn the search algorithm into an *anytime* algorithm that starts with a large approximation factor, computes an initial solution fast, and then progressively decreases the approximation factor at the expense of longer running times.

Indeed, we implemented an anytime version of T*ε, which we call *Anytime*-T*ε. Here, the first value of ε is defined as a very large number, e.g., $\varepsilon = 1000$, and we assume that the algorithm is given an upper bound on its overall running time. When Anytime-T*ε finds a solution and does not exceed the bound on the computation time, the value of ε is reduced, and a new search begins with smaller ε,

and with the already-computed transitions (which allows re-using the computation performed in the previous iterations). The new value of ε is determined using (i) the cost of the best-found solution that minimizes execution time and (ii) the cost of the best-found Dubins path with minimum speed. These serve as upper and lower bound for the cost of an optimal path, respectively:

$$\varepsilon_{new} = \frac{c(\gamma_{\mathsf{T}^*\varepsilon_{\text{old}}})}{c(\gamma_{\text{SP}}^{v_{\min}})}. \tag{6.1}$$

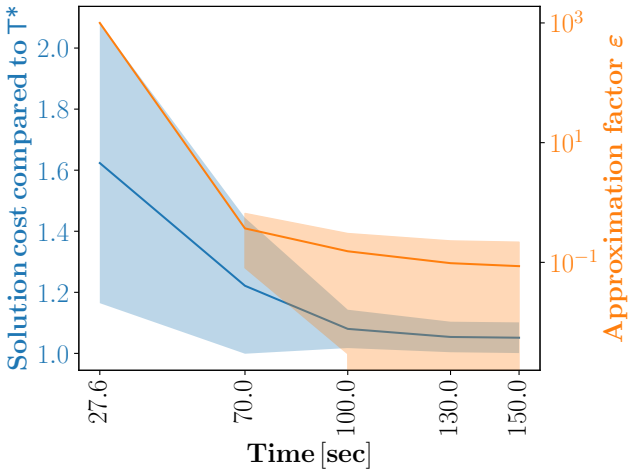

Figure 6.1: Anytime-$\mathsf{T}^*\varepsilon$ in dynamic environmental conditions with wind $\mathbf{w} = 0.2\hat{x} + 0\hat{y}$. Solution cost compared to T^* (blue) and approximation factors values (orange) as a function of the computational time.

We present in Fig. 6.1 preliminary results obtained by running Anytime-$\mathsf{T}^*\varepsilon$ averaged over 20 experiments. In the tested scenario, T^*'s running time is dominated by the computation of time-optimal transitions that last 400 seconds. As we found, starting with an extremely large approximation factor allows Anytime-$\mathsf{T}^*\varepsilon$ to obtain an initial solution roughly 14× faster than T^*. The cost of this initial solution is only 1.6× the cost of the optimal solution. Furthermore, as Anytime-$\mathsf{T}^*\varepsilon$ reuses computation from previous search episodes, it can obtain an optimal solution roughly 2.25× faster than T^*.

7 Appendix

To consider the setting where we need to account for wind currents, we detail the updated dynamics model and present two approaches to compute lower bounds on transitions cost-efficiently.

7.1 Updated Model

We assume that there is a constant wind $\mathbf{w} = (w_x, w_y)$ that changes the original system dynamics (Eq. 3.1) to

$$\begin{pmatrix} \dot{x}(t) \\ \dot{y}(t) \\ \dot{\theta}(t) \end{pmatrix} = \begin{pmatrix} v(t)\cos\theta(t) + w_x \\ v(t)\sin\theta(t) + w_y \\ u(t) \end{pmatrix}. \tag{7.1}$$

Furthermore, we assume that regardless of the magnitude of the wind, the vehicle will move forward. It is ensured by the additional assumption that the wind

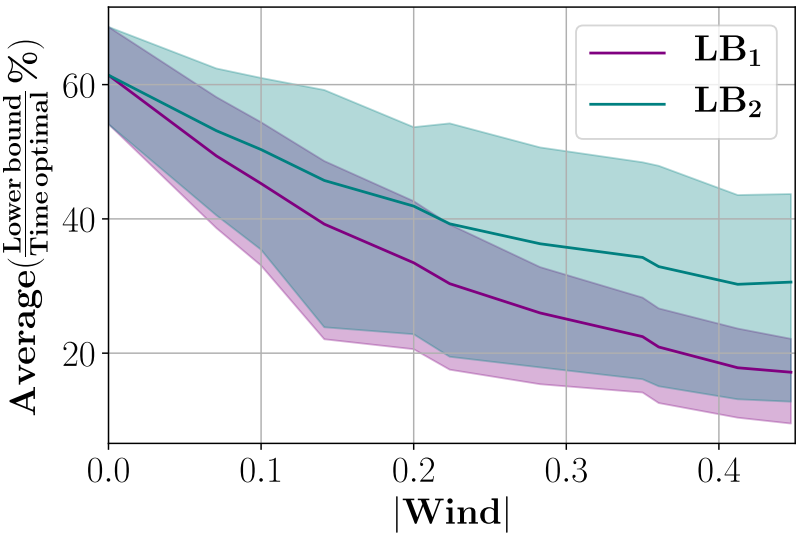

Figure 7.1: Average ratio between each lower bound and the time-optimal cost as a function of the wind's modulus (solid lines). Colored regions represent a 60% non-parametric confidence interval of the true value.

magnitude is smaller than the minimum speed of the system $v_{\min}$, i.e.,

$$|\mathbf{w}| < v_{\min}. \tag{7.2}$$

7.2 Updated Lower Bounds

The wind component may significantly influence the turning capabilities (in the reference frame of the ground). The smallest turning radius is obtained when flying directly against the wind. We denote it by ρ_{LB}, the lower bound radius, and have that

$$\rho_{\mathrm{LB}} = \left(1 - \frac{|\mathbf{w}|}{v_{\min}}\right) \rho_{\min}. \tag{7.3}$$

To this end, a lower bound on the true length of the path between two configurations s_1 and s_2 can be determined based on the length $\mathcal{L}(s_1, s_2, \rho_{\mathrm{LB}})$ of Dubins path with the lower bound radius ρ_{LB}. Now, if this value is divided by an upper bound on the effective maximal speed $v_{\max}^{\text{effective}}$ in the reference frame of the ground, it provides a lower bound on the true cost (i.e., the travel time).

We suggest two lower bounds based on how $v_{\max}^{\text{effective}}$ is determined. The first approach assumes that $v_{\max}^{\text{effective}} = v_{\max} + |\mathbf{w}|$. Namely, the effective maximal speed is the sum of the system's maximum speed and the wind magnitude. Thus, the first lower bound LB_1 is defined as

$$\mathrm{LB}_1(s_1, s_2) = \frac{\mathcal{L}(s_1, s_2, \rho_{\mathrm{LB}})}{v_{\max} + |\mathbf{w}|}. \tag{7.4}$$

The second lower bound LB_2 considers the direction between the start and end configurations (s_1 and s_2, respectively) by computing the ground speed $\mathbf{v}_{\mathrm{G}}$ in the given direction $\mathbf{d}$. The direction is determined based on s_1 and s_2 as

$$\mathbf{d} = \frac{s_2^{\mathrm{xy}} - s_1^{\mathrm{xy}}}{|s_2^{\mathrm{xy}} - s_1^{\mathrm{xy}}|}, \tag{7.5}$$

where s_i^{xy} stands for the x, y coordinates of the configuration s_i. The ground speed $\mathbf{v}_{\mathrm{G}}$ vector can be expressed by the system's aerial speed $\mathbf{v}$ and wind $\mathbf{w}$ as

$$\mathbf{v}_{\mathrm{G}} = \mathbf{v} + \mathbf{w}. \tag{7.6}$$

Following Eq. 7.2, the maximum ground speed occurs at the system's maximum

speed, i.e., $|\mathbf{v}| = v_{\max}$. The angle between $\mathbf{v}_{\mathrm{G}}$ and $\mathbf{w}$ can be written as

$$\cos \angle(\mathbf{v}_{\mathrm{G}}, \mathbf{w}) = \frac{\mathbf{d} \cdot \mathbf{w}}{|\mathbf{w}|}. \tag{7.7}$$

Subsequently, the ground speed can be expressed using the cosine rule as

$$|\mathbf{v}_{\mathrm{G}}| = \mathbf{d} \cdot \mathbf{w} + \sqrt{(\mathbf{d} \cdot \mathbf{w})^2 + v_{\max}^2 - |\mathbf{w}|^2}. \tag{7.8}$$

Finally, the second lower bound LB_2 is defined as

$$\mathrm{LB}_2(s_1, s_2) = \frac{\mathcal{L}(s_1, s_2, \rho_{\mathrm{LB}})}{|\mathbf{v}_{\mathrm{G}}|}. \tag{7.9}$$

Fig. 7.1 shows the average ratio between each lower bounds and the true cost as a function of the wind force. For both lower bounds, their estimation of the true cost becomes looser as the wind force increases. Notice that LB_2 is more informative than LB_1 because accounting for the direction enables reducing the upper bound on the ground speed. In addition, notice that both lower bounds reduce to the system's minimum-speed Dubins path divided by the maximum speed in static environmental conditions. Thus, we used LB_2 as lower bound for dynamic environmental conditions.

Bibliography

[1] J. Song, S. Gupta, and T. A. Wettergren, "T*: Time-optimal risk-aware motion planning for curvature-constrained vehicles," *RA-L*, vol. 4, no. 1, pp. 33–40, 2018.

[2] L. B. Kratchman, M. M. Rahman, J. R. Saunders, P. J. Swaney, and R. J. Webster III, "Toward robotic needle steering in lung biopsy: a tendon-actuated approach," in *Medical Imaging: Visualization, Image-Guided Procedures, and Modeling*, vol. 7964, 2011, p. 79641I.

[3] H. Xiang and L. Tian, "Development of a low-cost agricultural remote sensing system based on an autonomous unmanned aerial vehicle (UAV)," *Biosystems Engineering*, vol. 108, no. 2, pp. 174–190, 2011.

[4] D. Sadigh, S. Sastry, S. A. Seshia, and A. D. Dragan, "Planning for autonomous cars that leverage effects on human actions," in *RSS*, vol. 2, 2016, pp. 1–9.

[5] B. Garau, M. Bonet, A. Alvarez, S. Ruiz, and A. Pascual, "Path planning for autonomous underwater vehicles in realistic oceanic current fields: Application to gliders in the western mediterranean sea," *J. Marit. Res.*, vol. 6, no. 2, pp. 5–22, 2009.

[6] P. K. Agarwal, T. Biedl, S. Lazard, S. Robbins, S. Suri, and S. Whitesides, "Curvature-constrained shortest paths in a convex polygon," *SIAM J. Comput.*, vol. 31, no. 6, pp. 1814–1851, 2002.

[7] Z. Zeng, L. Lian, K. Sammut, F. He, Y. Tang, and A. Lammas, "A survey on path planning for persistent autonomy of autonomous underwater vehicles," *O.E.*, vol. 110, pp. 303–313, 2015.

[8] N. Wang, D. Zhang, L. Zhou, and Q. Liu, "Near optimal path planning for vehicle with heading and curvature constraints," in *WCICA*, 2010, pp. 4514–4519.

[9] J. Pearl and J. H. Kim, "Studies in semi-admissible heuristics," *IEEE Trans. Pattern Anal. Mach. Intell*, no. 4, pp. 392–399, 1982.

[10] R. Bohlin and L. E. Kavraki, "Path planning using lazy PRM," in *ICRA*, vol. 1, 2000, pp. 521–528.

[11] K. Hauser, "Lazy collision checking in asymptotically-optimal motion planning," in *ICRA*, 2015, pp. 2951–2957.

[12] C. Dellin and S. Srinivasa, "A unifying formalism for shortest path problems with expensive edge evaluations via lazy best-first search over paths with edge selectors," in *ICAPS*, vol. 26, no. 1, 2016.

[13] A. Mandalika, S. Choudhury, O. Salzman, and S. Srinivasa, "Generalized lazy search for robot motion planning: Interleaving search and edge evaluation via event-based toggles," in *ICAPS*, vol. 29, 2019, pp. 745–753.

[14] J. Ketchel and P. Larochelle, "Collision detection of cylindrical rigid bodies for motion planning," in *ICRA*, 2006, pp. 1530–1535.

[15] N. Haghtalab, S. Mackenzie, A. Procaccia, O. Salzman, and S. Srinivasa, "The provable virtue of laziness in motion planning," in *ICAPS*, vol. 28, no. 1, 2018.

[16] L. E. Dubins, "On curves of minimal length with a constraint on average curvature, and with prescribed initial and terminal positions and tangents," *Am. J. Math.*, vol. 79, no. 3, pp. 497–516, 1957.

[17] A. Wolek, E. M. Cliff, and C. A. Woolsey, "Time-optimal path planning for a kinematic car with variable speed," *J. Guid. Control Dyn.*, vol. 39, no. 10, pp. 2374–2390, 2016.

[18] K. Kučerová, P. Váňa, and J. Faigl, "On finding time-efficient trajectories for fixed-wing aircraft using dubins paths with multiple radii," in *Annual ACM Symposium on Applied Computing*, 2020, pp. 829–831.

[19] J. P. Wilson, Z. Shen, S. Gupta, and T. A. Wettergren, "T*-lite: A fast time-risk optimal motion planning algorithm for multi-speed autonomous vehicles," in *OCEANS MTS/IEEE*, 2020, pp. 1–6.

[20] E. Plaku, "Robot motion planning with dynamics as hybrid search," in *AAAI*, 2013.

[21] J. P. Wilson, K. Mittal, and S. Gupta, "Novel motion models for time-optimal risk-aware motion planning for variable-speed AUVs," in *OCEANS MTS/IEEE*, 2019, pp. 1–5.

[22] L. Techy and C. A. Woolsey, "Minimum-time path planning for unmanned aerial vehicles in steady uniform winds," *J. Guid. Control Dyn.*, vol. 32, no. 6, pp. 1736–1746, 2009.

[23] J. Faigl, P. Váňa, M. Saska, T. Báča, and V. Spurnỳ, "On solution of the dubins touring problem," in *ECMR*, 2017, pp. 1–6.

[24] R. Pěnička, J. Faigl, and M. Saska, "Physical orienteering problem for unmanned aerial vehicle data collection planning in environments with obstacles," *RA-L*, vol. 4, no. 3, pp. 3005–3012, 2019.

[25] P. E. Hart, N. J. Nilsson, and B. Raphael, "A formal basis for the heuristic determination of minimum cost paths," *IEEE Trans. Syst. Man Cybern.*, vol. 4, no. 2, pp. 100–107, 1968.

[26] K. Mittal, J. Song, S. Gupta, and T. A. Wettergren, "Rapid path planning for dubins vehicles under environmental currents," *IEEE Robot. Autom. Mag.*, vol. 134, p. 103646, 2020.

[27] S. Koenig, M. Likhachev, and D. Furcy, "Lifelong planning A*," *Artif. Intell.*, vol. 155, no. 1-2, pp. 93–146, 2004.

[28] R. Ebendt and R. Drechsler, "Weighted A* search–unifying view and application," *Artif. Intell.*, vol. 173, no. 14, pp. 1310–1342, 2009.